Electronic Supplementary Material (ESI) for Chemical Communications

Capture of Iodine in highly stable Metal-Organic Frameworks: a systematic study

Clément Falaise,[†] Christophe Volkringer,[*, †] Jacques Facqueur, [†] Till Bousquet, [†] Laurent Gasnot,[‡] Thierry Loiseau[†]

[†]Unité de Catalyse et Chimie du Solide (UCCS) – UMR CNRS 8181, Université de Lille Nord de France-ENSCL, Bat. C7, BP 90108, 59652 Villeneuve d'Ascq, France

[‡]Physicochimie des Processus de Combustion et de l'Atmosphère (PC2A) – UMR CNRS 8522, Université de Lille Nord de France, 59655 Villeneuve d'Ascq, France

* To whom correspondence should be addressed. E-mail: christophe.volkringer@ensc-lille.fr. Phone:
(33) 3 20 434 973, Fax: (33) 3 20 43 48 95

Supplementary information

To be submitted to Chem. Comm.
Version May 13, 2013

Selected MOFs.

Table S1: Porous characteristics of MOFs used in this study.

MOF	Formula (hydrated solid)	Type of porosity	Swelling	BET surface (m^2/g)
MIL-53-X	Al(OH)bdc-X·H_2O (X = H, Cl, Br, CH_3, NH_2, NO_2, $(OH)_2$, COOH, $(COOH)_2$	1D channel (∅ ≈ 8Å)	Yes	Up to 1140 (X = H)
MIL-96	$Al_{12}O(OH)_{18}(H_2O)_3(Al_2(OH)_4(btc)_6 \cdot 2H_2O$	Microporous cavities (∅≈ 8-14 Å) Microporous windows (∅≈ 2-4 Å)	No	487
MIL-100	$Al_3O(OH)(H_2O)_2(btc)_4 \cdot 16H_2O$	Mesoporous cavities (∅≈ 25-29 Å) Microporous window (∅≈ 5-9 Å)	No	2152
MIL-101-NH_2	$Al_3O(OH)_2(H_2O)_2(bdc\text{-}NH_2)_3 \cdot nH_2O$	Mesoporous cavities (∅≈ 25-29 Å) Microporous window (∅≈ 5-9 Å)	No	2100
MIL-118	$Al_2(OH)_2(btec) \cdot 2.75H_2O$	1D channel (∅ ≈ 4Å)	Yes	/
MIL-120	$Al_4(OH)_8(btec) \cdot 5.3H_2O$	1D channel (∅ ≈ 6Å)	No	308
CAU-1	$Al_4(OH)_2(OMe)_4(bdc\text{-}NH_2)3 \cdot 3H_2O$	Microporous cavities (∅ ≈ 5-10 Å)	No	1434

Abrevation :

- bdc : 1,4-benzenedicarboxylate (or terephthalate)
- btc : 1,3,5-benzentricarboxylate (or trimesate)
- btec : 1,2,4,5-benzentetracraboxylic acid (or pyromellitate)

References for selected Al-Based MOFs:

MIL-53-H: T. Loiseau, C. Serre, C. Huguenard, G. Fink, F. Taulelle, M. Henry, T. Bataille, G. Férey, *Chem. Eur. J.* **2004**, 10, 1373.

MIL-53-NH_2: T. Ahnfeldt, D. Gunzelmann, T. Loiseau, D. Hirsemann, J. Senker, G. Férey, N. Stock, *Inorg. Chem.* **2009**, 48, 3057.

MIL-53-X (X = -Cl, -Br, -CH_3, -NO_2, -$(OH)_2$): S. Biswas, T. Ahnfeldt, N. Stock, *Inorg. Chem*. **2011**, 50, 9518.

MIL-53-COOH: N. Reimer, B. Gil, B. Marszalek, N. Stock, *CrystEngComm.* **2012**, 14, 4119.

MIL-53-$(COOH)_2$: C. Volkringer, T. Loiseau, N. Guillou, G. Férey, M ; Haouas, F. Taulelle, E. Elkaim, N. Stock, *Inorg. Chem.* **2010**, 49, 9852.

MIL-96: T. Loiseau, L. Lecrocq, C. Volkringer, J. Marrot, G. Férey, M. Haouas, F. Taulelle, S. Bourelly, P.L. Llewellyn, M. Latroche, *J. Am. Chem. Soc*. **2006**, 128, 10223.

MIL-100: C. Volkringer, D. Popov, T. Loiseau, G. Férey, M. Burghammer, C. Riekel, M. Haouas, F. Taulelle, *Chem. Mater*. **2009**, 21, 5695.

MIL-101-NH_2: P. Serra-Crespo, E.V. Ramos-Fernandez, J. Gascon, F. Kapteijn, *Chem. Mater.* **2011**, 23, 2565.

MIL-118c: C. Volkringer, T. Loiseau, N. Guillou, G. Férey, M. Haouas, F. Taulelle, N. Audebrand, I. Margiolaki, D. Popov, M. Burghammer, C. Riekel, *Cryst. Growth Des.* **2009**, 9, 2927

MIL-120: C. Volkringer, T. Loiseau, M. Haouas, F. Taulelle, D. Popov, M. Burghammer, C. Riekel, C. Zlotea, F. Cueavas, M. Latroche, D. Phanon, C. Kofelv, P.L. Llewellyn, G. Férey, *Chem. Mater.* **2009**, 21, 5783

CAU-1: T. Ahnfeldt, N. Guillou, D. Gunzelmann, I. Margiolaki, T. Loiseau, G. Férey, J. Senker, N. Stock, *Angew. Chem. Int. Ed.* **2009**, 48, 5163

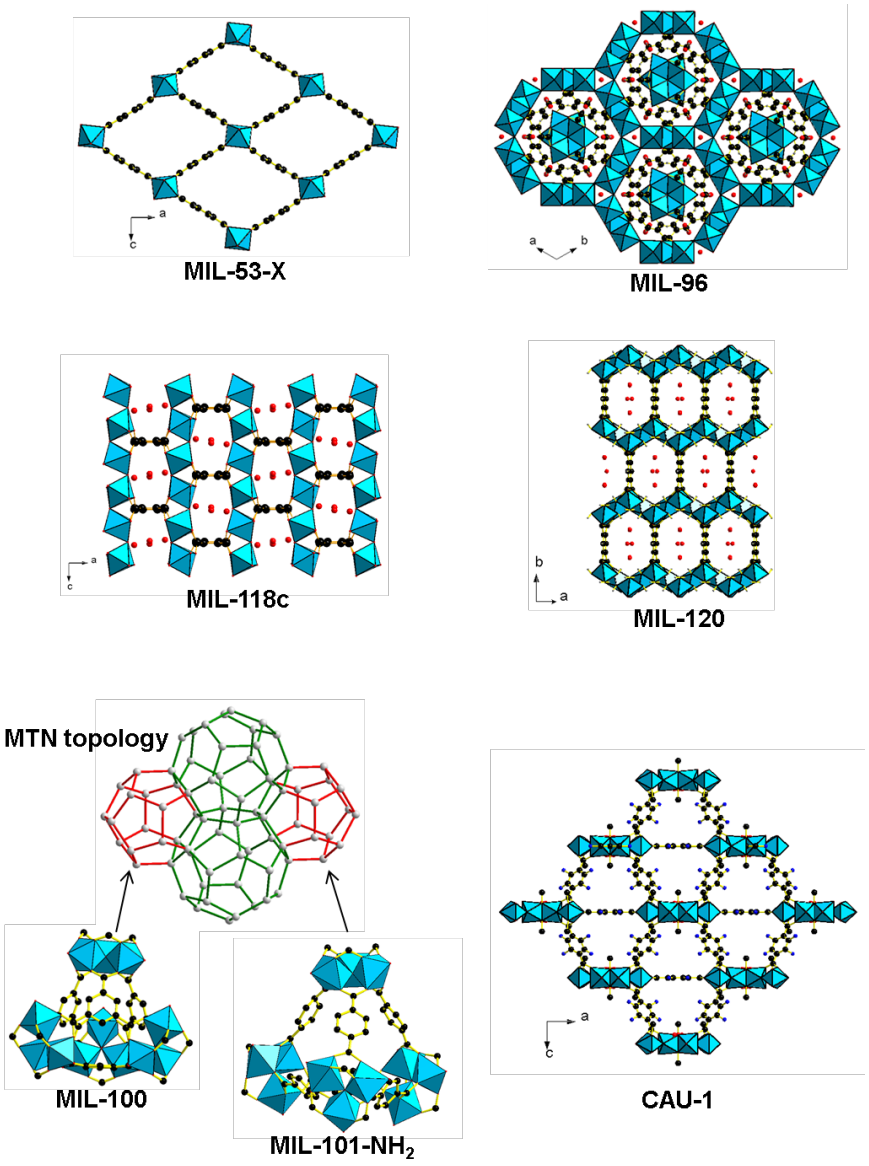

Figure S1. Illustrations of the selected Al-based MOFs.

Powder X-Ray diffraction patterns of selected MOFs before and after I2 loading

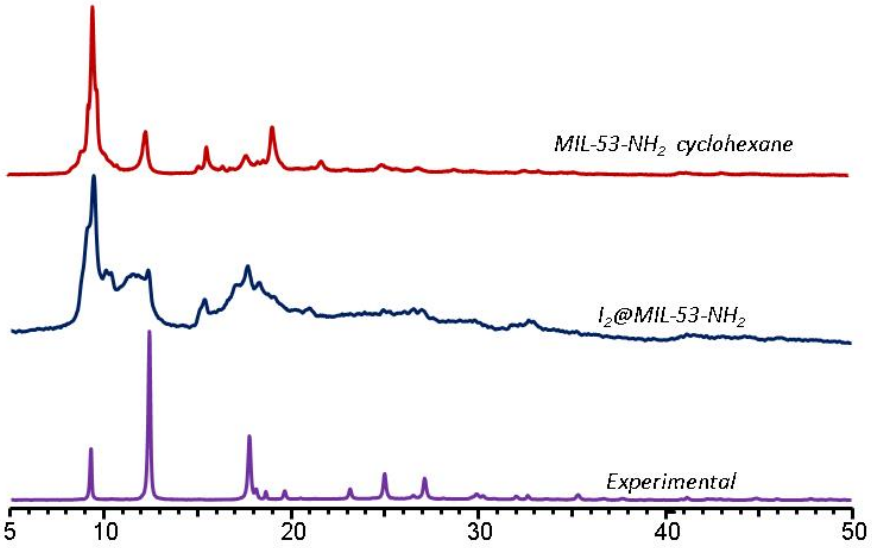

Figure S2a. Comparison between powder x-ray diffraction patterns of the as-synthesized, the I_2 loaded MIL-53-(NH_2) and MIL-53-NH_2 in contact with cyclohexane.*

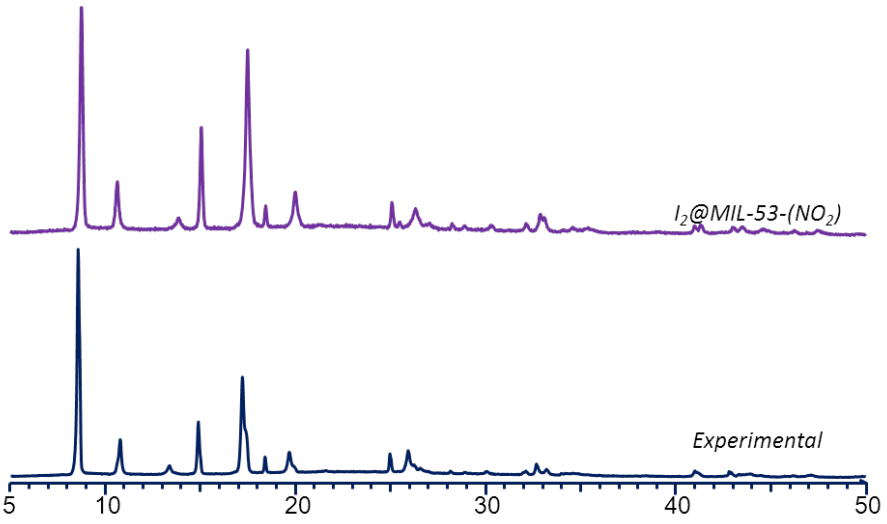

Figure S2b. Comparison between powder x-ray diffraction patterns of the as-synthesized and the I_2 loaded MIL-53-(NO_2).*

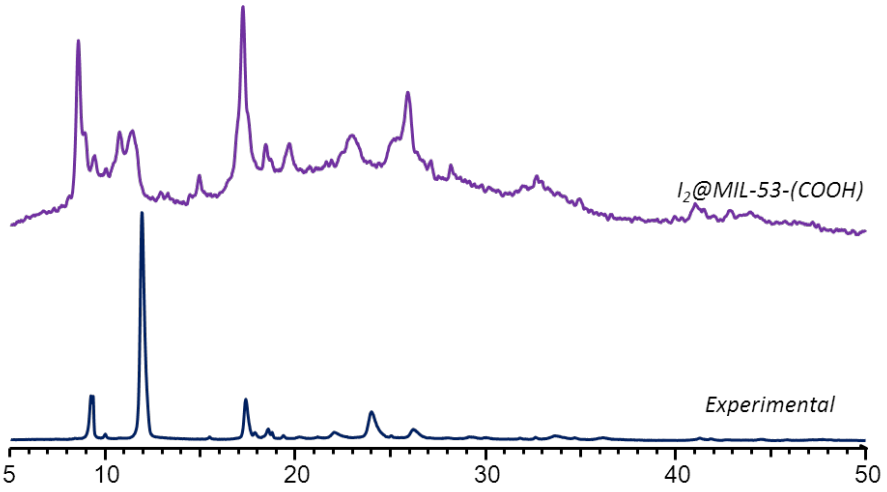

Figure S2c. Comparison between the powder x-ray diffraction patterns of as-synthesized and the I_2 loaded MIL-53-(COOH).*

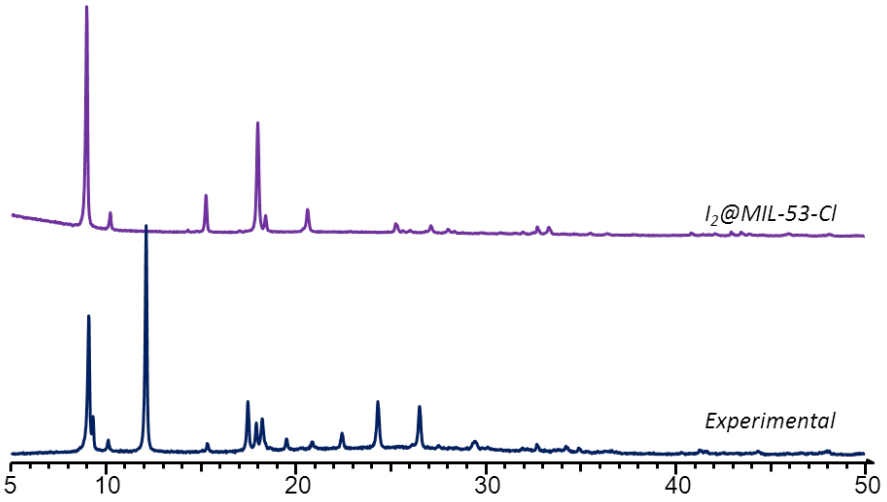

Figure S2d. Comparison between the powder x-ray diffraction patterns of as-synthesized and the I_2 loaded MIL-53-(Cl).*

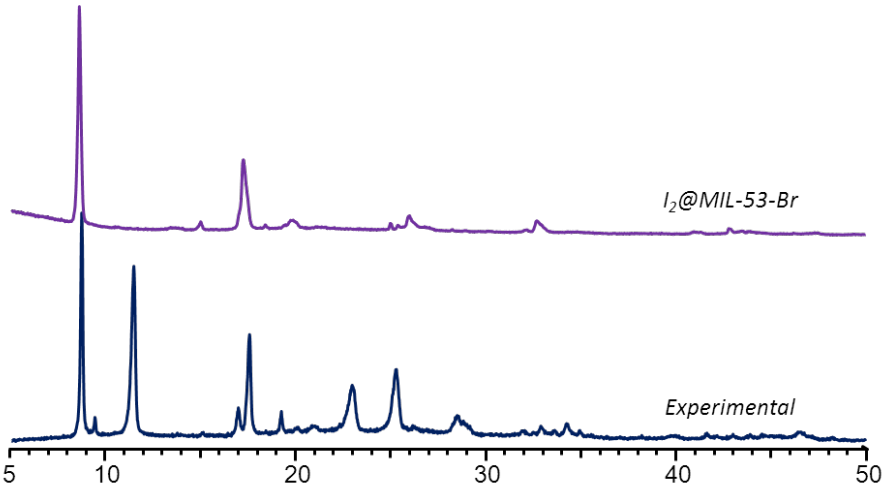

Figure S2e. Comparison between the powder x-ray diffraction patterns of as-synthesized and the I_2 loaded MIL-53-(Br).*

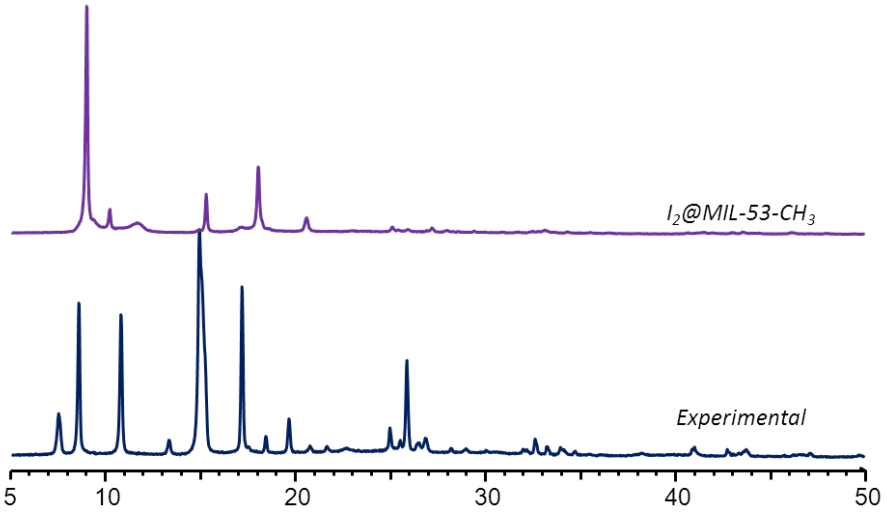

Figure S2f. Comparison between the powder x-ray diffraction patterns of as-synthesized and the I_2 loaded MIL-53-(CH_3).*

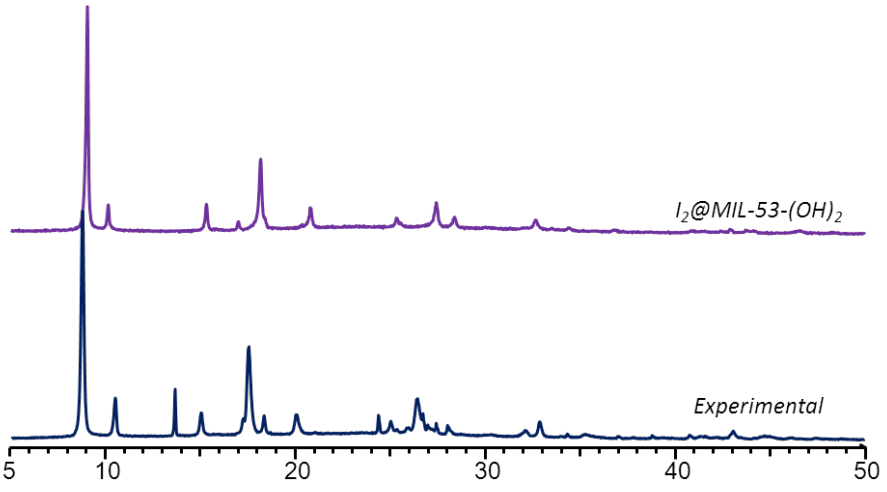

Figure S2g. Comparison between the powder x-ray diffraction patterns of as-synthesized and the I_2 loaded MIL-53-$(OH)_2$.*

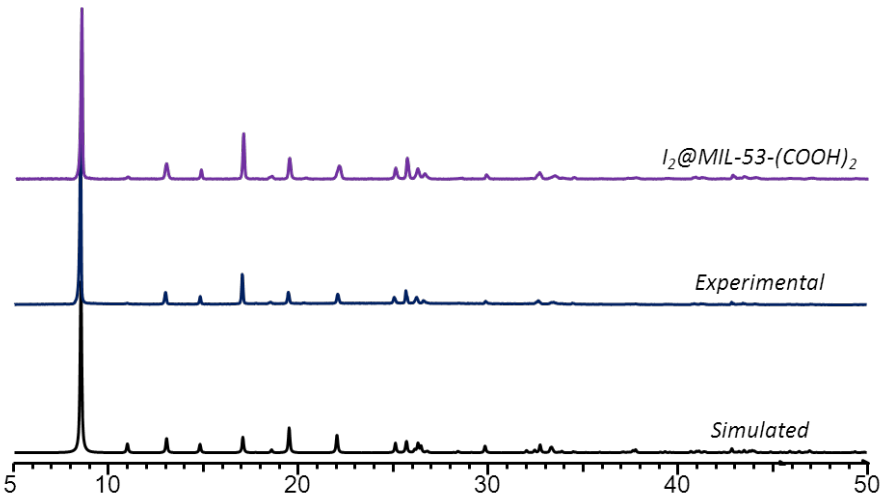

Figure S2h. Comparison between the powder x-ray diffraction patterns of as-synthesized and the I_2 loaded MIL-53-$(COOH)_2$.

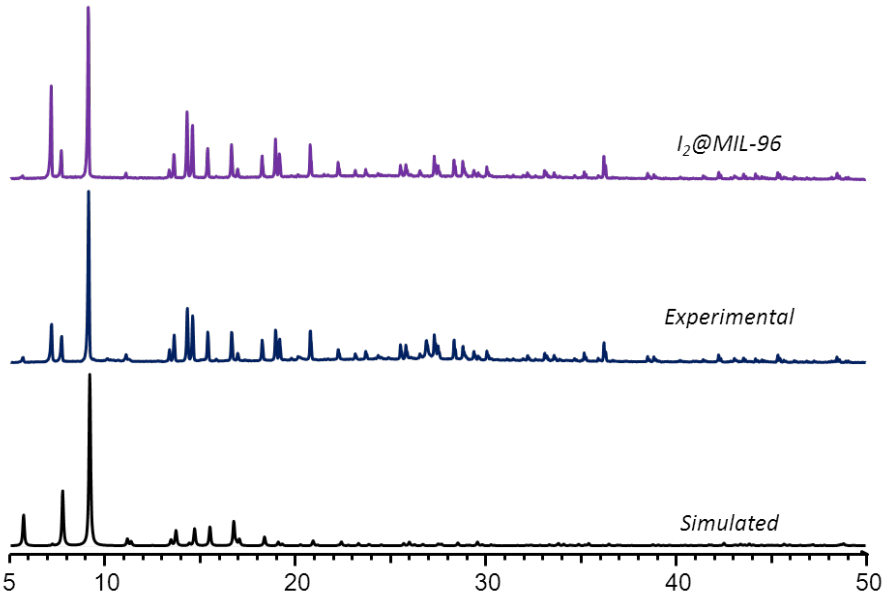

Figure S2i. Comparison between the powder x-ray diffraction patterns of as-synthesized and the I_2 loaded MIL-96.

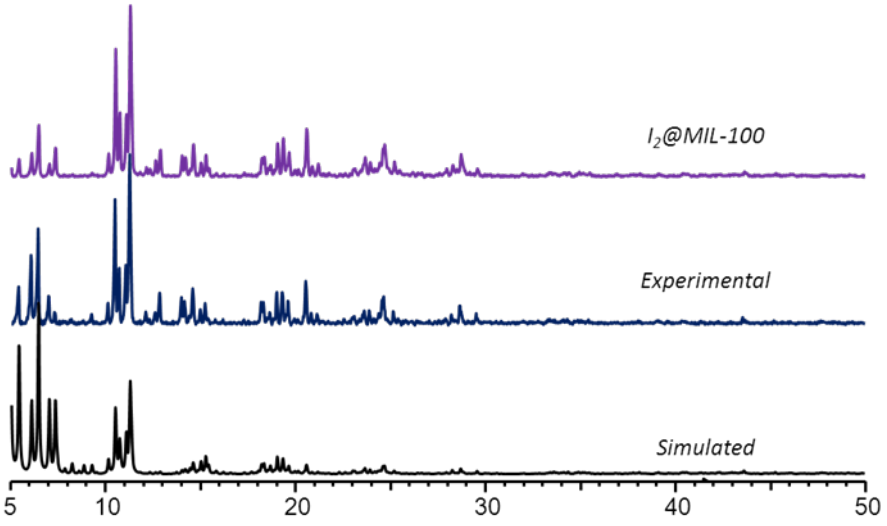

Figure S2j. Comparison between the powder x-ray diffraction patterns of as-synthesized and the I_2 loaded MIL-100.

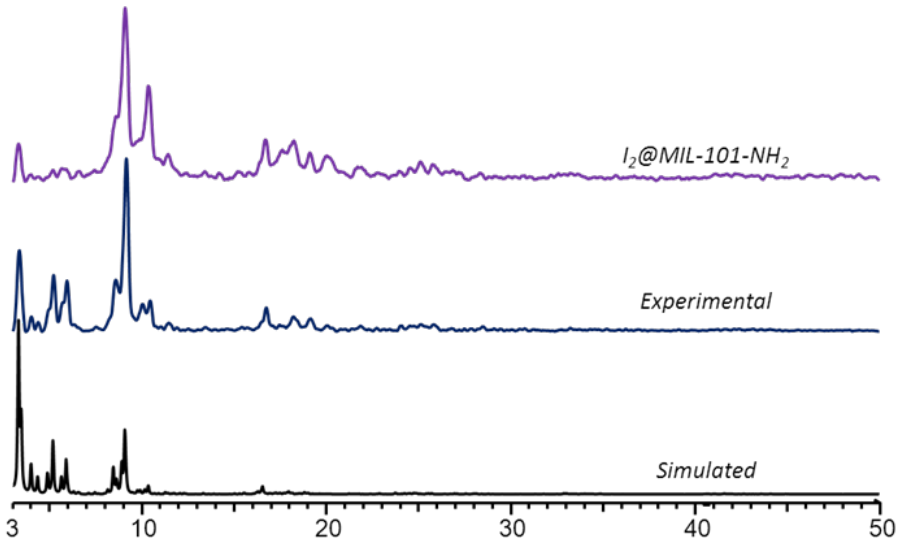

Figure S2k. Comparison between the powder x-ray diffraction patterns of as-synthesized and the I_2 loaded MIL-101-NH_2.

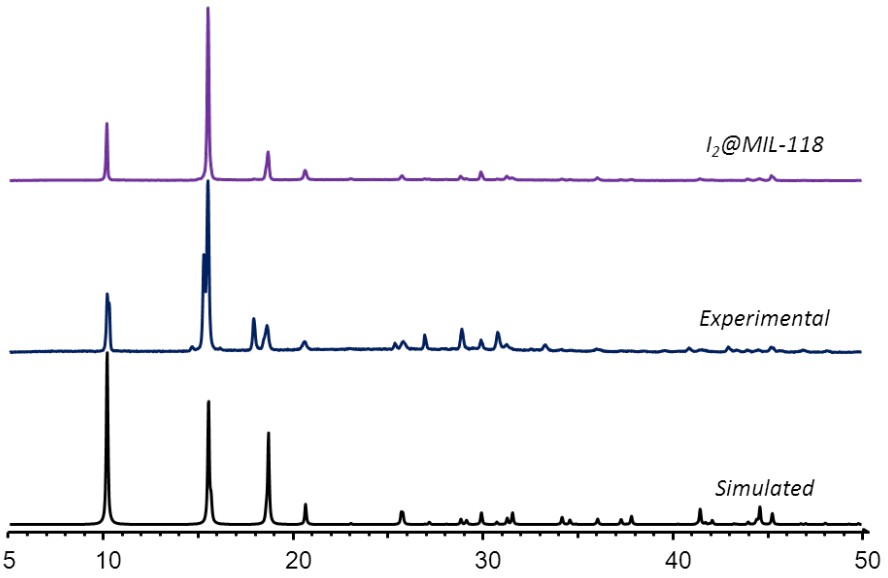

Figure S2l. Comparison between the powder x-ray diffraction patterns of as-synthesized and the I_2 loaded MIL-118.

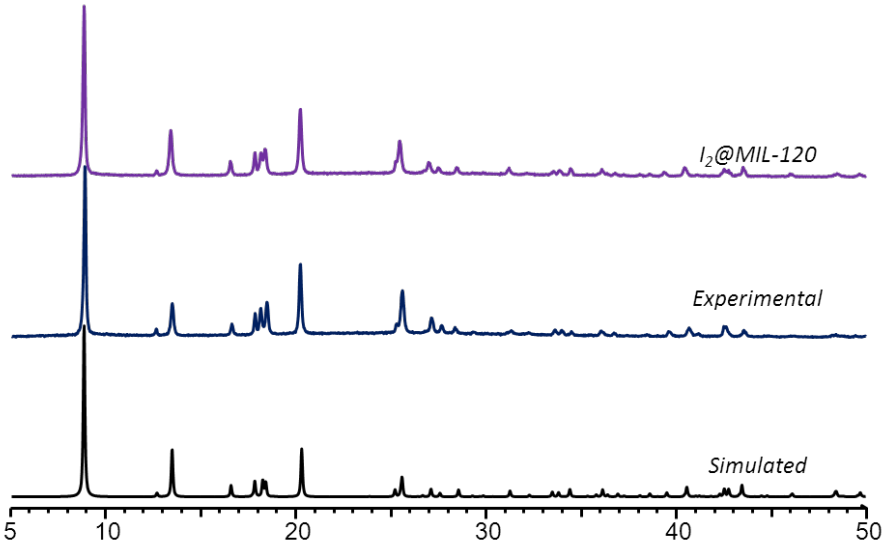

Figure S2m. Comparison between the powder x-ray diffraction patterns of as-synthesized and the I_2 loaded MIL-120.

* Some MILn compounds have no reported simulated XRD patterns in the literature and therefore were not shown.

UV/vis spectroscopy

UV/Vis spectra have been carried out on a Perkin Elmer Lambda 650 spectrophotometer within the wavelength range 200–700 nm, using the same solvent in the analyzed solution as a blank. A powder sample holder set was equipped for the characterization of solids.
The evolution UV/vis spectrum for iodine in cyclohexane solution shows two absorption peaks λ_1= 223 nm and λ_2=523 nm. The intensity of absorption peaks (peaks λ_1= 223 nm and λ_2=523 nm) was proportional with the quantity of I_2. The curve of calibration was obtained by four solutions (0.025, 0.05, 0.076, 0.101 mg/l).

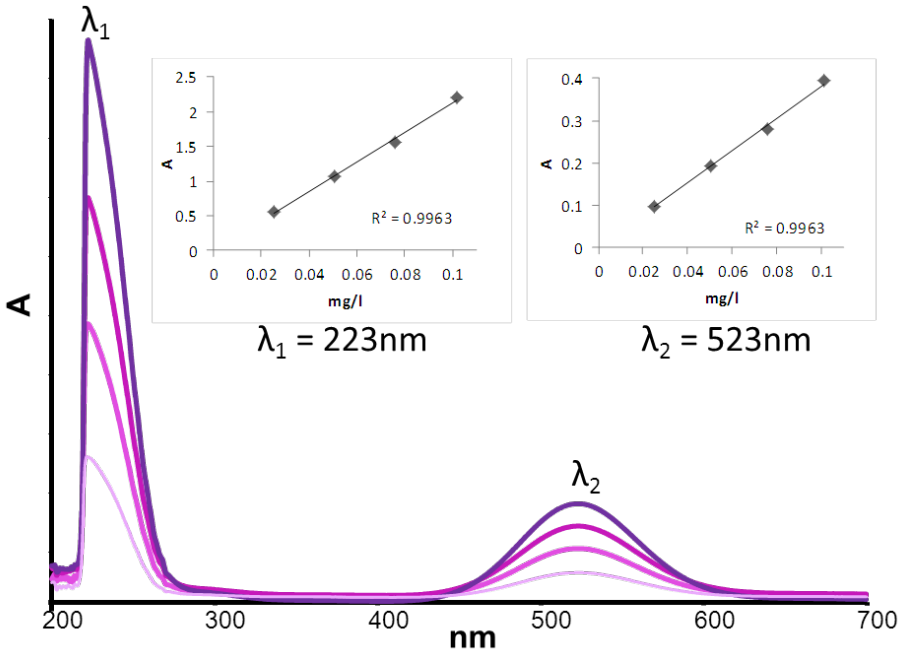

Figure S3a. Calibration plot of iodine in cyclohexane by UV/vis spectrum.

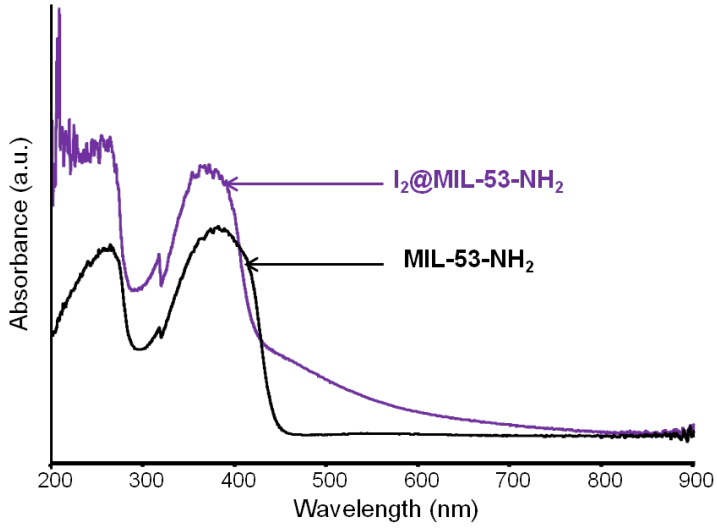

Figure S3b. Comparison between solid state UV/Vis spectra of the as-synthesized and the I_2 loaded MIL-53-(NH_2).

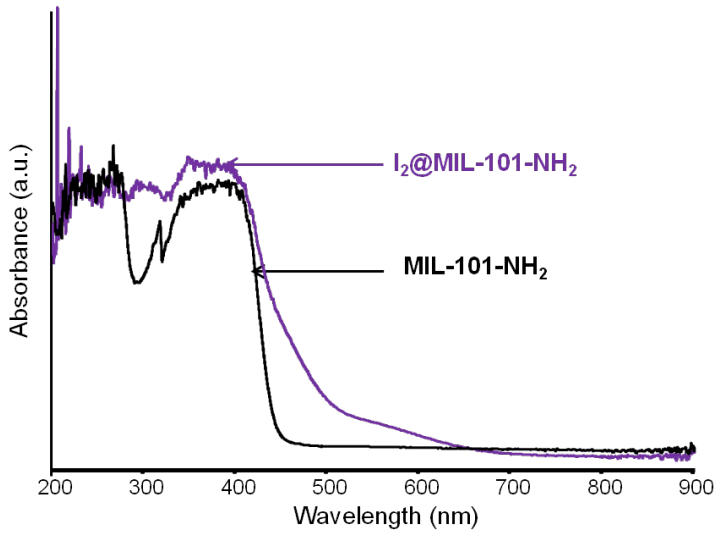

Figure S3c. Comparison between solid state UV/Vis spectra of the as-synthesized and the I_2 loaded MIL-101-(NH_2).

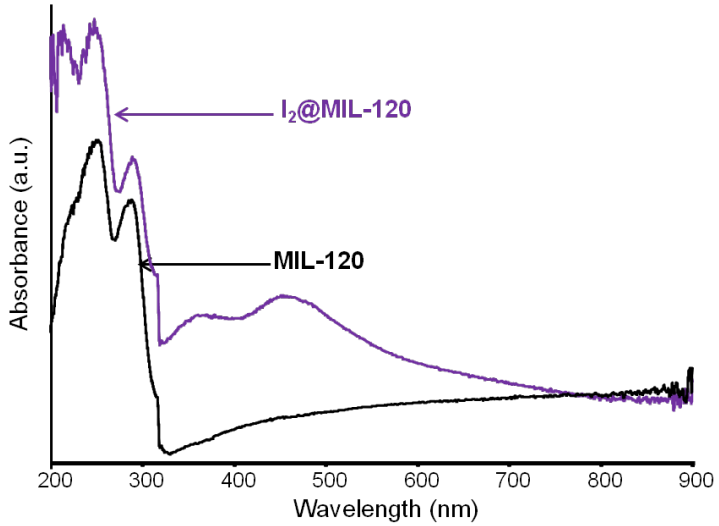

Figure S3d. Comparison between solid state UV/Vis spectra of the as-synthesized and the I_2 loaded MIL-120.

In the case of I_2@MIL-120, the band centered around 350 cm^{-1} is characteristic for a charge transfer complex involving iodine I_2 [see for instance the same observation reported by R.J. Session *et al. Chem. Phys. Letters* 242 177-183 (1995)]. Unfortunately, this band is hidden by ligand absorption bands in MIL-53-NH_2 and MIL-101-NH_2.

Photography

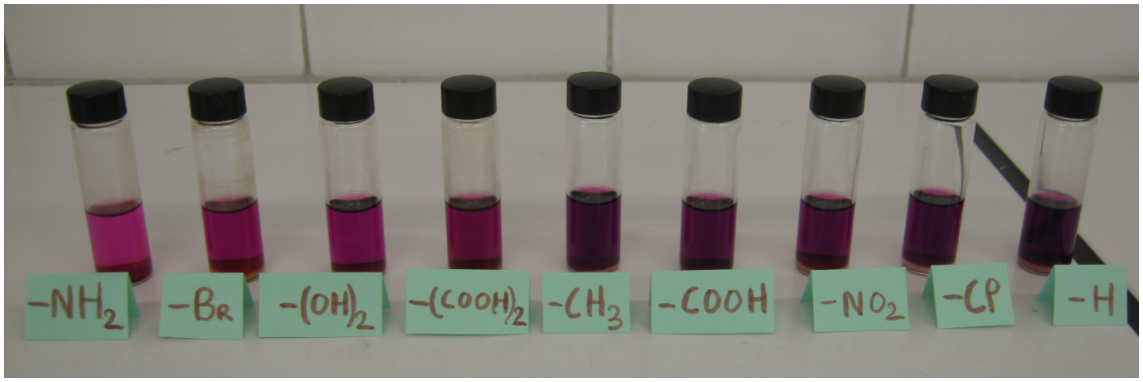

Figure S4a. Picture showing the visual color change after adsorption of iodine through the MIL-53 family (C_i=0.01M, t =48h and T°=RT).

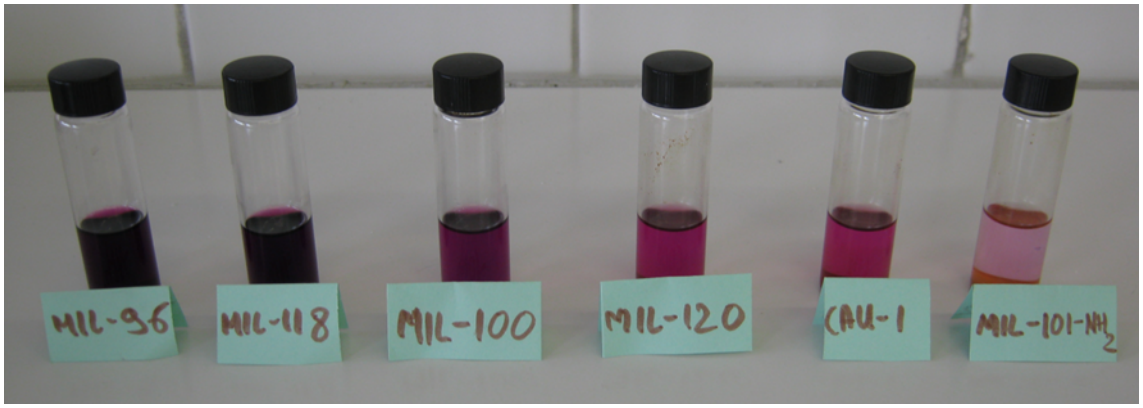

Figure S4b. Picture showing the visual color change after adsorption of iodine with rigid MOFs MIL-96, MIL-100, MIL-101-NH_2, MIL-118, MIL-120 and CAU-1 (C_i=0.01M, t =48h and T°=RT).

Sorption kinetics.

Adsorption experiments

The removal efficiency was calculated by using the following equation.

$$Removal\ (\%) = \frac{(C_i - C_{e(or\ t)})}{C_i} \times 100$$

The amount of I_2 adsorbed was defined by the following equation.

$$q_{e(t)} = \frac{V(C_i - C_{e(t)})}{m}$$

Where C_t and C_e are the concentration at time t and at equilibrium (mg/l), C_i is the initial concentration of I_2 in cyclohexane (mg/l), q_t and q_e are the amount of I_2 adsorbed at time t and equilibrium (mg/g), m is the mass of MOF powder used (g).

Pseudo first order kinetic model

The linear form of pseudo first order kinetic model is expressed by the following equation.

$$\log(q_e - q_t) = \log q_e - \frac{k_1}{2.303} t$$

Where q_e and q_t are previously defined, k_1 is the pseudo first order rate constant for the adsorption process (min^{-1}).

Table S2. Parameters of the pseudo first order kinetic models extracted from experimental data for MIL-53-NH_2, MIL-53-Br, MIL-53-$(OH)_2$, MIL-53-$(COOH)_2$, MIL-100, MIL-120, MIL-101-NH_2 and CAU-1.

	Intercept	Slope	k_1	R^2
MIL-53-NH_2	1.6832	-0.0446	0.1027138	0.9116
MIL-53-Br	1.623	-0.0384	0.0884352	0.9086
MIL-53-$(OH)_2$	1.6907	-0.0202	0.0465206	0.9473
MIL-53-$(COOH)_2$	1.6476	-0.0345	0.0794535	0.9934
MIL-100	1.5712	-0.0288	0.0663264	0.9712
MIL-120	1.8547	-0.0553	0.1273559	0.9516
MIL-101-NH_2	1.7794	-0.0545	0.1255135	0.9704
CAU-1	1.79	-0.0502	0.1156106	0.976

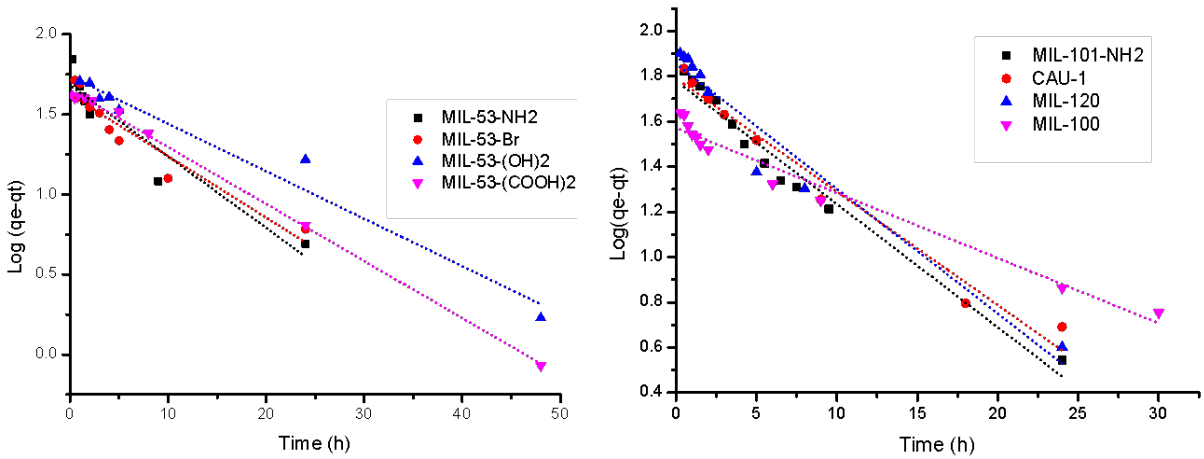

Figure S5.Plots of pseudo-first order kinetics for the adsorption of I_2 in cyclohexane on some MIL-53-X (X = -$(COOH)_2$, -$(OH)_2$, -Br, NH_2) series and rigid MOFs (MIL-100, MIL-101-NH2, MIL-120 and CAU-1).

Pseudo second order kinetic model

The linear form of pseudo second order kinetic model is expressed by the following equation.

$$\frac{t}{q_t} = \frac{1}{k_2 {q_e}^2} + \frac{1}{q_e} t$$

Where q_e and q_t are previously defined, k_2 is the pseudo second order rate constant for the adsorption process (g/mg min).

Table S3. Parameters of the pseudo-second order kinetic models extracted from experimental data for MIL-53-NH_2, MIL-53-Br, MIL-53-$(OH)_2$, MIL-53-$(COOH)_2$, MIL-100, MIL-120, MIL-101-NH_2 and CAU-1.

	Intercept	Slope	*qe*	k_2	R^2
MIL-53-NH_2	0.02457	0.01273	78.5545954	0.00659556	0.99862
MIL-53-Br	0.05848	0.01558	64.1848524	0.00415076	0.99821
MIL-53-$(COOH)_2$	0.1609	0.02006	49.8504487	0.00250095	0.97607
MIL-53-$(OH)_2$	0.1225	0.01524	65.6167979	0.00189598	0.97961
MIL-100	0.04318	0.01806	55.3709856	0.00755358	0.99265
MIL-120	0.01412	0.00892	112.107623	0.00563501	0.99911
MIL-101-NH_2	0.01132	0.00787	127.064803	0.00547146	0.99929
CAU-1	0.01619	0.00913	109.529025	0.00514867	0.99903

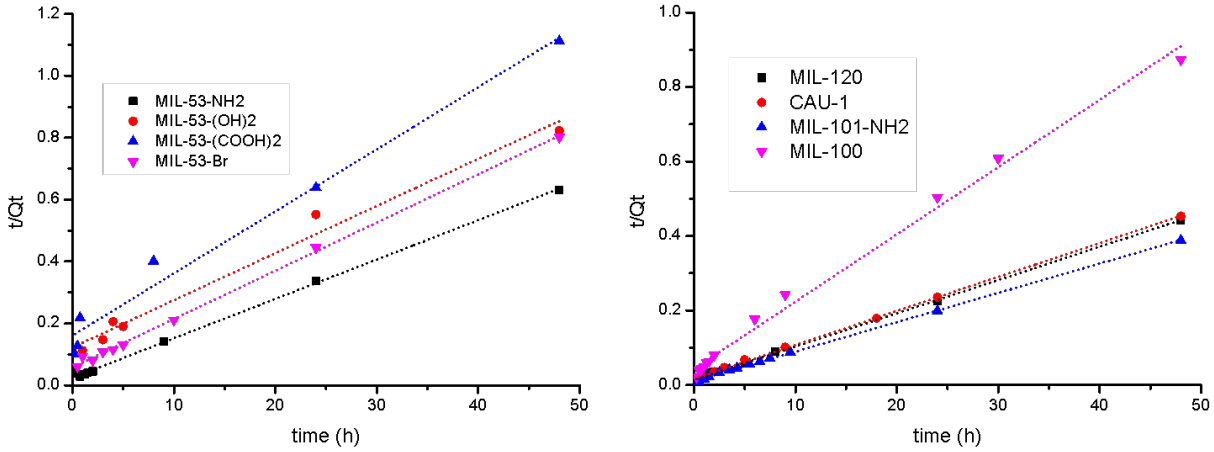

Figure S6.Plots of pseudo-second order kinetics for the adsorption of I2 in cyclohexane on some MIL-53-X (X = -$(COOH)_2$, -$(OH)_2$, -Br, NH_2) series and rigid MOFs (MIL-100, MIL-101-NH2, MIL-120 and CAU-1).

Intra-particle diffusion model

The linear form of pseudo second order kinetic model is expressed by the following equation.

$$q_t = k_i t^{1/2} + C$$

Where q_e, q_t and t are previously defined, k_i is the pseudo second order rate constant for the adsorption process (g/mg min) and C is the intercept (mg/g).

Table S4. Parameters of the intraparticle kinetic models extracted from experimental data for MIL-53-NH_2, MIL-53-Br, MIL-53-$(OH)_2$, MIL-53-$(COOH)_2$, MIL-100, MIL-120, MIL-101-NH_2 and CAU-1.

	k_i	C	R^2
MIL-NH_2	9.33751	21.42022	0.76397
MIL-53-Br	8.02454	12.50852	0.79774
MIL-53-$(COOH)_2$	7.07423	-2.49842	0.96077
MIL-$(OH)_2$	8.1413	3.22207	0.96295
MIL-100	6.70952	12.94172	0.94108
MIL-120	13.3867	32.97796	0.79491
MIL-101-NH_2	11.00695	62.87848	0.76097
CAU-1	11.28462	42.31061	0.83756

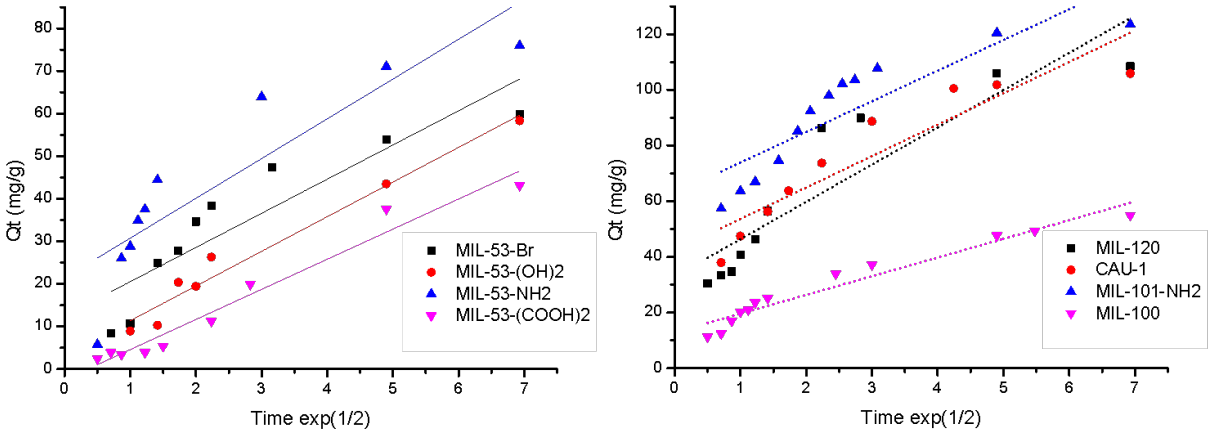

Figure S7.Intraparticle diffusion plot for the adsorption of I_2 in cyclohexane on some MIL-53-X (X = -$(COOH)_2$, -$(OH)_2$, -Br, NH_2) series and rigid MOFs (MIL-100, MIL-101-NH2, MIL-120 and CAU-1).

Effect of hydration

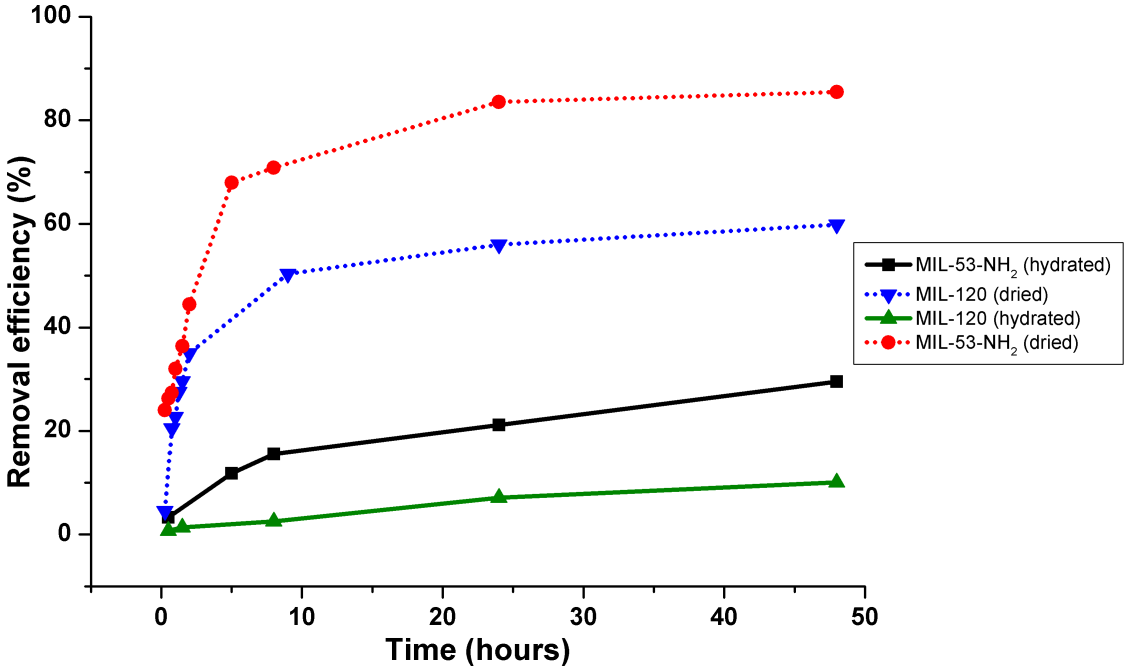

Figure S8. Comparison of iodine adsorption kinetics between dried and hydrated versions of MIL-53(Al)-NH_2 and MIL-120(Al).

I_2 releasing for selected I_2@MOF compounds in ethanol

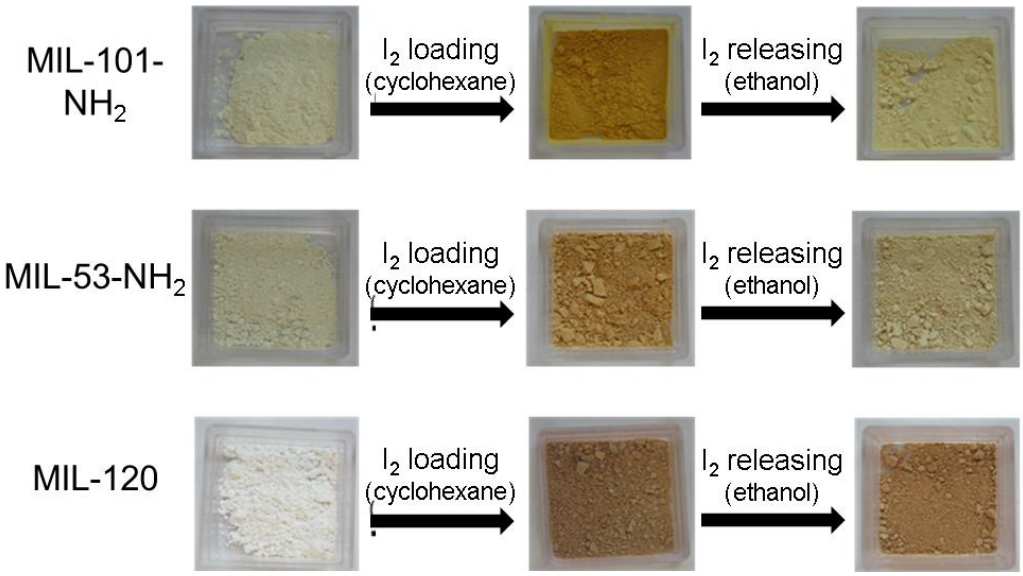

Figure S9a. Optical observation of powdered MOFs upon loading and releasing I_2.

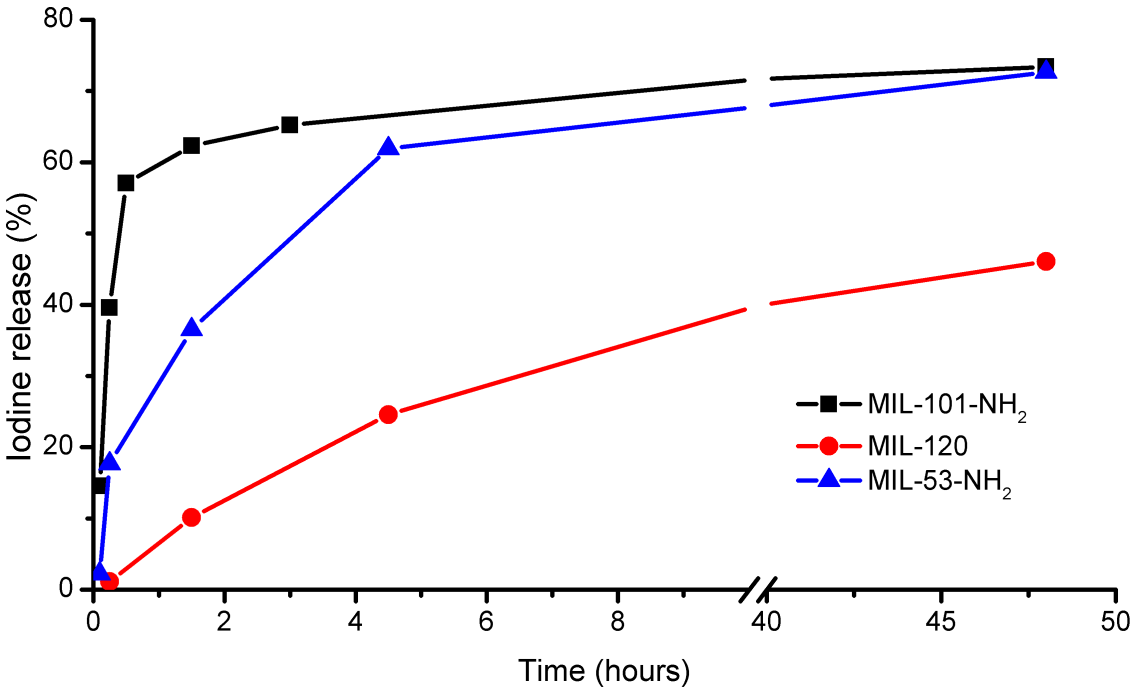

Figure S9b. Release of I_2 in ethanol from iodine charged MIL-53(Al)-NH_2, MIL-101(Al)-NH_2 and MIL-120(Al), as a function of time.

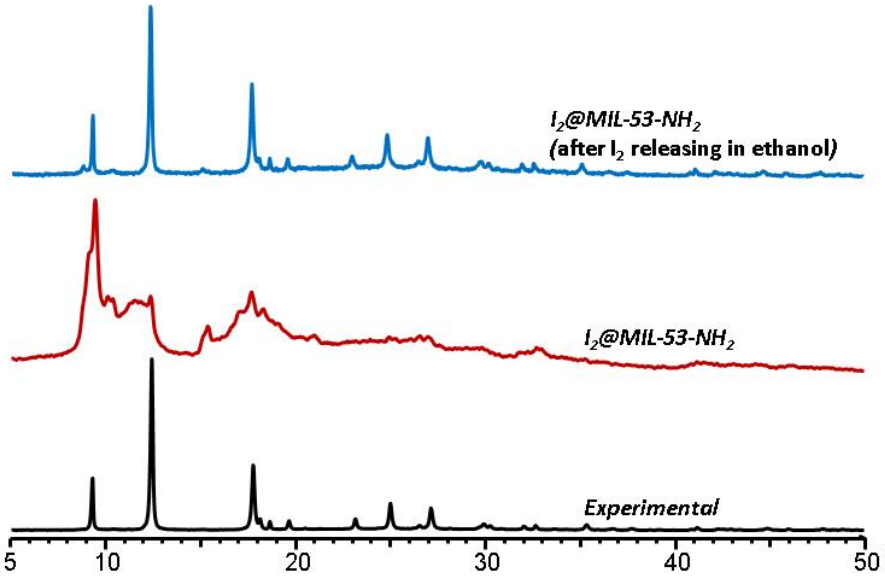

Figure S9c. Comparison between powder x-ray diffraction patterns of the as-synthesized, I_2 loaded MIL-53-NH_2 and I_2 loaded MIL-53-NH_2 after I_2 releasing in ethanol.

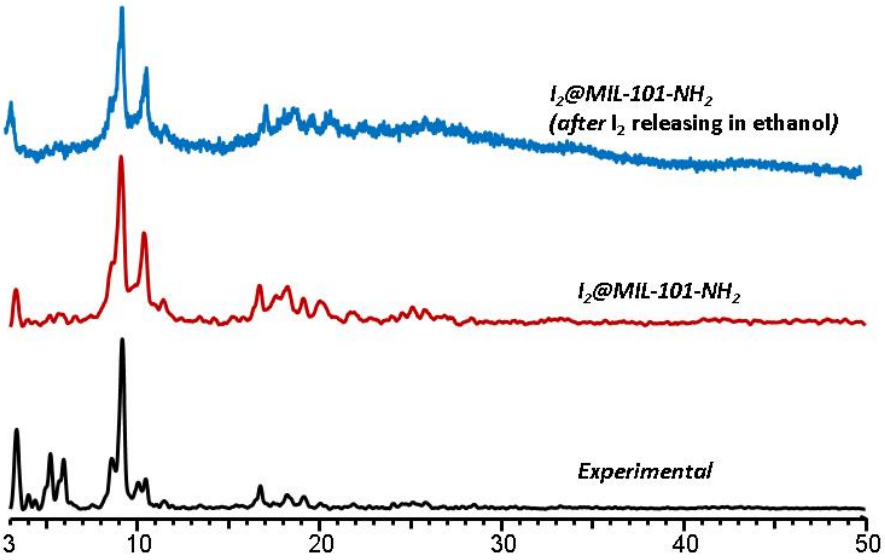

Figure S9d. Comparison between powder x-ray diffraction patterns of the as-synthesized, I_2 loaded MIL-101-NH_2 and I_2 loaded MIL-101-NH_2 after I_2 releasing in ethanol.

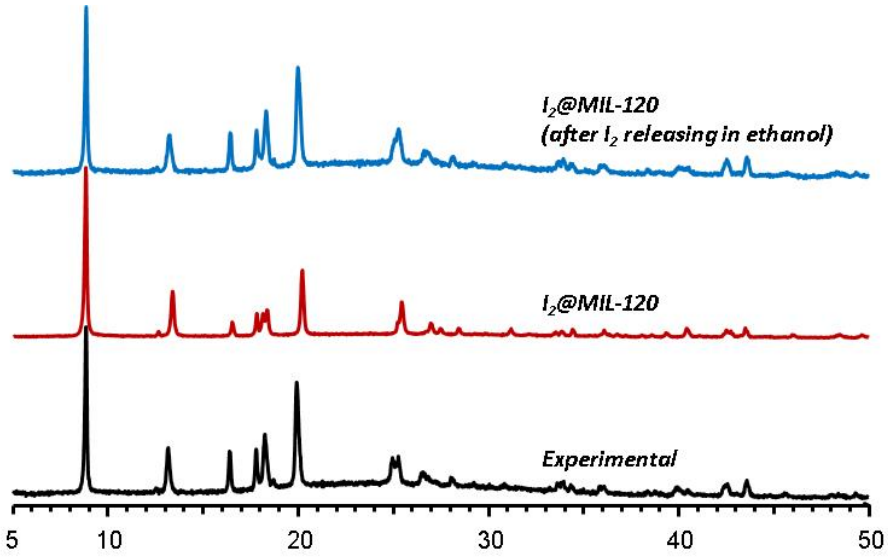

Figure S9e. Comparison between powder x-ray diffraction patterns of the as-synthesized I_2, loaded MIL-120 and I_2 loaded MIL-120 after I_2 releasing in ethanol.

Sorption equilibrium

Langmuir isotherrm

The equation of Langmuir is expressed by the following equation.

$$q_e = \frac{k_L C_e}{1 + a_L C_e}$$

Where q_e and C_e are previously defined, k_L (l/g) and a_L (l/mg) are the Langmuir isotherm constants.

Table S5. Parameters of the Langmuir isotherm models extracted from experimental adsorption isotherms data for MIL-101-NH_2, CAU-1, MIL-53-NH_2, MIL-120 and MIL-100.

	K_L		a_L		Statistics
	Value	Standard Error	Value	Standard Error	R^2
MIL-101-NH_2	1.20573	0.35461	0.00316	0.00116	0.92237
CAU-1	0.29392	0.06748	7.66E-04	2.71E-04	0.94407
MIL-53-NH_2	0.21222	0.01113	9.86E-04	7.70E-05	0.9951
MIL-120	0.94414	0.29102	0.00583	0.00211	0.93108
MIL-100	0.55637	0.05563	0.00857	9.93E-04	0.98818

Freundlich isotherm

The equation of Freundlich is expressed by the following equation.

$$q_e = k_F C_e^{\,1/n_F}$$

Where q_e and C_e are previously defined, k_F (l/g) and a_F (l/mg) are the Freundlich isotherm constants.

Table S6. Parameters of the Freundlich isotherm models extracted from experimental adsorption isotherms data for MIL-101-NH_2, CAU-1, MIL-53-NH_2, MIL-120 and MIL-100.

	K_F		n_F		Statistics
	Value	Standard Error	Value	Standard Error	R^2
MIL-101-NH_2	25.42398	3.49353	3.0146	0.17065	0.99021
CAU-1	4.7209	0.98128	2.00016	0.10878	0.99137
MIL-53-NH_2	3.82981	0.95649	2.15569	0.15381	0.97883
MIL-120	17.36029	4.9153	3.59894	0.49838	0.94711
MIL-100	10.80519	3.64895	4.38114	0.92269	0.83753

Redlich-Peterson isotherm

The equation of Langmuir is expressed by the following equation.

$$q_e = \frac{a_r C_e}{(1 + k_r {C_e}^{\beta})}$$

Where q_e and C_e are previously defined, a_r, k_r and β are the Redlich-Peterson isotherm constants.

Table S7. Parameters of the Redlich-Peterson isotherm models extracted from experimental adsorption isotherms data for MIL-101-NH_2, CAU-1, MIL-53-NH_2, MIL-120 and MIL-100.

	a_r		k_r		β		Statistics
	Value	Standard Error	Value	Standard Error	Value	Standard Error	R^2
MIL-101-NH_2	13.4205	10.05276	0.39862	0.36774	0.70333	0.0256	0.99457
CAU-1	7.30044	47.20785	1.38444	9.95964	0.51233	0.08308	0.98866
MIL-53-NH_2	0.27619	0.03512	0.00517	0.00317	0.83671	0.0578	0.99786
MIL-120	2.7648	1.50045	0.07286	0.06385	0.81948	0.04803	0.98108
MIL-100	0.6333	0.09285	0.01287	0.00443	0.96379	0.02886	0.98962

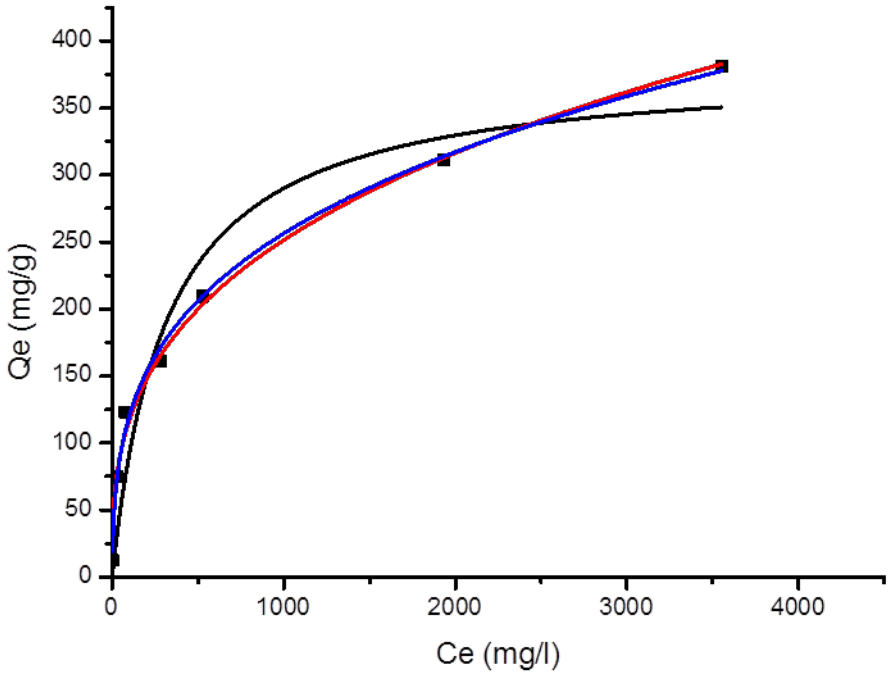

Figure S10a. Comparison of Langmuir (black line), Freundlich (red line) and Redlich-Peterson (blue line) isotherms for sorption of I_2 into MIL-101-NH_2.

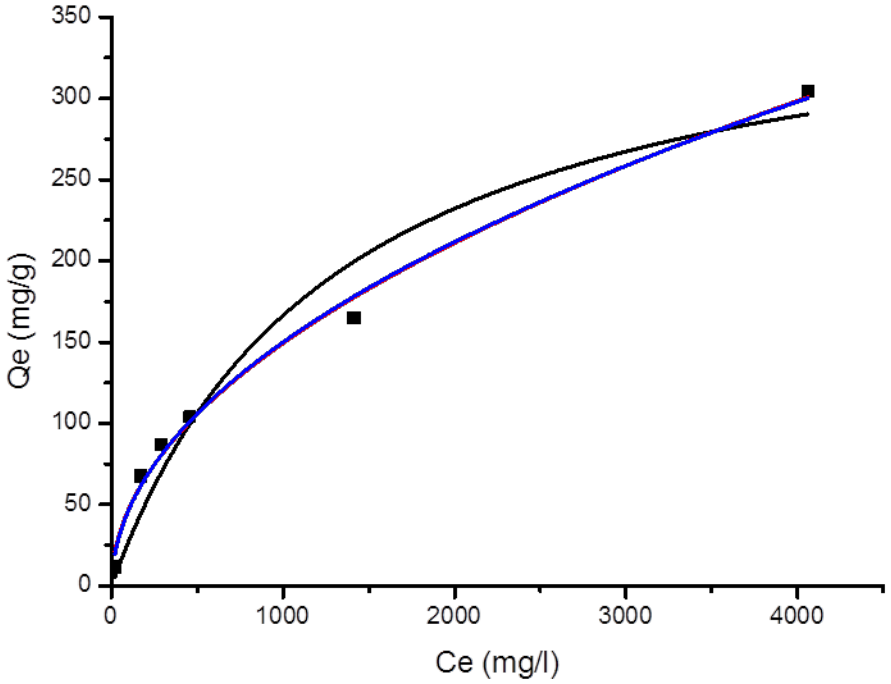

Figure S10b. Comparison of Langmuir (black line), Freundlich (red line) and Redlich-Peterson (blue line) isotherms for sorption of I_2 into CAU-1.

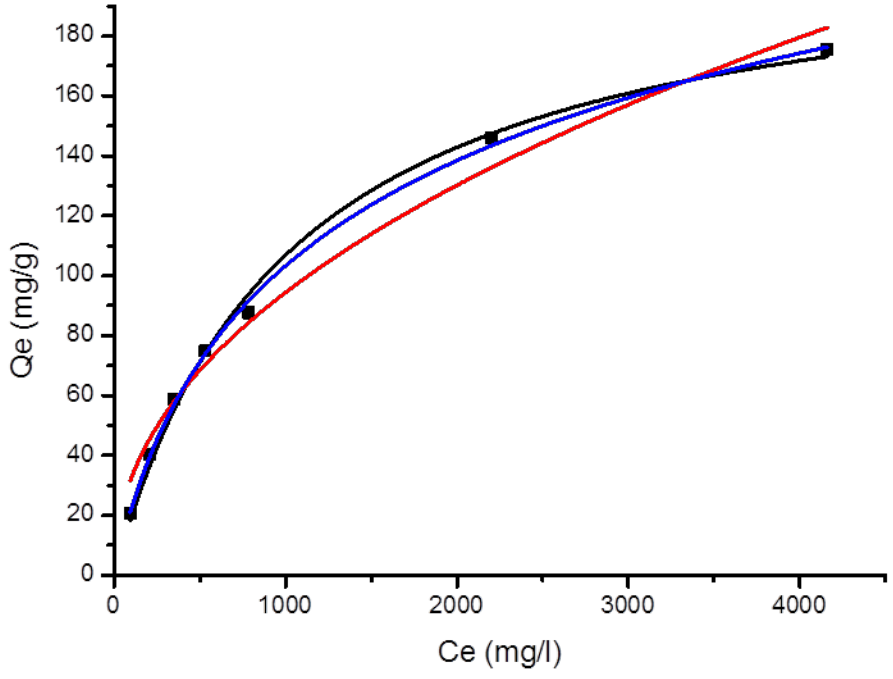

Figure S10c. Comparison of Langmuir (black line), Freundlich (red line) and Redlich-Peterson (blue line) isotherms for sorption of I_2 into MIL-53-NH_2.

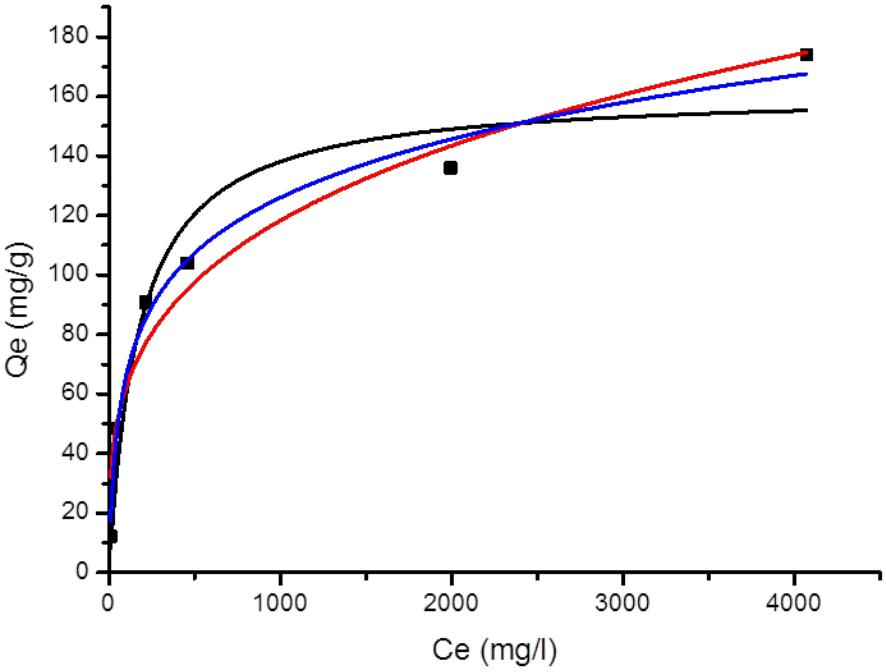

Figure S10d. Comparison of Langmuir (black line), Freundlich (red line) and Redlich-Peterson (blue line) isotherms for sorption of I_2 into MIL-120.

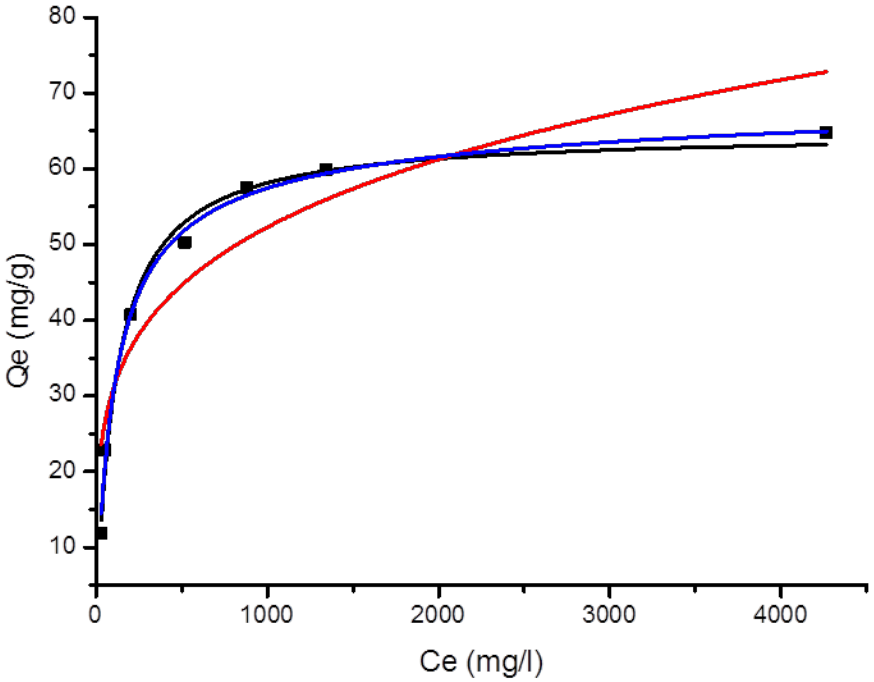

Figure S10e. Comparison of Langmuir (black line), Freundlich (red line) and Redlich-Peterson (blue line) isotherms for sorption of I_2 into MIL-100.

Sample loadings

Table S8: Sample iodine loadings of MIL-53-NH_2, MIL-100, MIL-101-NH_2, MIL-120 and CAU-1, calculated at Ci = 0.01 M (48h) and after partial I2 releasing in ethanol, by UV-vis spectroscopy and ICP-MS spectroscopy.

	Loading (5ml; C_i= 0,01M; 48h)		Release (5ml; ethanol ; 48h)	
	Qd (mg/g, **UV**)	Qd (mg/g, **ICP-MS**)	Qd (mg/g, **UV**)	Qd (mg/g, **ICP-MS**)
MIL-101-NH_2	124	121	31	20
MIL-120	108	106	63	61
MIL-53-NH_2	76	73	20	17

Table S9: Sample iodine loading of MIL-53-NH_2, MIL-100, MIL-101-NH_2, MIL-120 and CAU-1 and comparison with the corresponding MOF porosity and functional group concentration.

	I_2 Loading (from UV/Vis) (5ml; C_e= 3500mg/l; 48h)		BET surface (m^2/g)	Functional group concentration (mmol per gram of MOF)
	I/Al	I/NH_2 (or OH for MIL-120)		
CAU-1	0.45	0.60	1434	3.70 (-NH_2)
MIL-53-NH_2	0.29	0.29	< 1000	4.48 (-NH_2)
MIL-101-NH_2	0.71	0.71	2100	2.87 (-NH_2)
MIL-120	0.10	0.05	308	16.19 (-OH)